Geospatial Solutions for Urban Climate Adaptation: The LCZ-UHI-GEO Project between Italy and Vietnam

Matej Žgela [1], Alberto Vavassori [1], Maria Antonia Brovelli [1], Giovanna Venuti [1], Deodato Tapete [2], Patrizia Sacco [2], Pham Thi Mai Thy [3], Lam Dao Nguyen [3]

[1] Department of Civil and Environmental Engineering, Politecnico di Milano, Milano, Italy - (matej.zgela, alberto.vavassori, maria.brovelli, giovanna.venuti)@polimi.it
[2] Italian Space Agency (ASI), Rome, Italy – (deodato.tapete, patrizia.sacco)@asi.it
[3] Vietnam National Space Center (VNSC), Ho Chi Minh City, Vietnam – (ldnguyen, ptmthy)@vnsc.org.vn

Keywords: Local Climate Zones, Urban Heat Island, Air Temperature Mapping, PRISMA Hyperspectral satellite, Urban Environments

Abstract:
The LCZ-UHI-GEO project is an international collaboration between Italy and Vietnam, aiming to analyse urban climate dynamics, particularly the Urban Heat Island (UHI) effect, through geospatial techniques. The project focuses on four major cities—Rome and Milan in Italy, and Hanoi and Ho Chi Minh City in Vietnam. The project's objectives include mapping Local Climate Zones (LCZ) using Earth Observation (EO) data and mapping high-resolution air temperature based on in-situ and EO data. A key highlight is the integration of hyperspectral (HS) imagery from the PRISMA satellite to improve LCZ classification accuracy compared to traditional multispectral (MS) data. This paper presents the first experiments carried out for LCZ mapping in Rome and air temperature mapping in Milan. In Rome, LCZ mapping achieved 88.1% overall accuracy using PRISMA imagery, outperforming Sentinel-2 data which obtained an accuracy of 73.7%. Air temperature mapping in Milan employed a machine learning (ML) based interpolation combining Sentinel-2 data, GIS data, in-situ official weather station data, and crowdsourced Netatmo sensor measurements. Temperatures were modelled for the summer of 2022 for five specific diurnal periods, namely 4-6 AM, 9-11 AM, 2-4 PM, 6-8 PM, and 9 PM-12 AM. The resulting high-resolution temperature maps revealed distinctive UHI patterns for each period, with peak intensity observed during night-time. The model performed well across different periods, achieving an average root mean square error (RMSE) of 1.4°C. Future work will expand PRISMA data collection and provide multi-temporal LCZ and temperature mapping, particularly in Vietnamese cities. By utilising advanced geospatial technologies, the LCZ-UHI-GEO project contributes to sustainable urban development and addresses the challenges of urbanisation and climate change.

1. Introduction

Urbanisation plays a critical role in local climate formation and significantly contributes to the man-made climate crisis (Chapman et al., 2017). With nearly 60% of the world's population living in cities, studying urban climates is increasingly important.

A major consequence of urbanisation is the UHI effect, where urban areas are warmer than their rural surroundings (Oke et al., 2017). This is caused by replacing natural surfaces with artificial materials such as asphalt and concrete, which heat up faster and retain less heat. Also, the UHI effect intensifies during heatwaves, leading to increased heat-related health risks, energy demand, and pressure on urban sustainability and planning.

Urban climates also vary within cities due to differences in neighbourhood structures and the mix of green and artificial surfaces. To address this variability, the concept of LCZs was introduced (Stewart and Oke, 2012). LCZs classify urban and suburban areas based on their physical and thermal properties. They are typically mapped using MS satellite imagery combined with morphological information on the built environment and vegetation and serve as invaluable tools for understanding urban heat dynamics and supporting sustainable urban planning.

In the framework of the recently concluded "Local Climate Zones in Open Data Cube" (LCZ-ODC) project, a collaboration between Politecnico di Milano and the Italian Space Agency (ASI), a novel methodology was proposed for LCZ mapping using HS imagery from the ASI's PRISMA (*Precursore IperSpettrale della Missione Applicativa*) satellite. Such an approach demonstrated that PRISMA imagery improves LCZ mapping accuracy compared to Sentinel-2 MS data. Given this result, the project "Analysis of Local Climate Zones and the Urban Heat Island through Geomatic Techniques" (LCZ-UHI-GEO) started in 2024 aiming to replicate and expand the methodologies developed in LCZ-ODC, focusing on major urban areas with diverse characteristics, i.e. Milan and Rome in Italy and Hanoi and Ho Chi Minh City in Vietnam. LCZ-UHI-GEO is an international collaboration funded by the Italian Ministry of Foreign Affairs and International Cooperation (MAECI) and Vietnam's Ministry of Science and Technology (MOST).

The project aims to generate detailed LCZ and air temperature maps through advanced geospatial techniques, contributing to the broader goals of sustainable urban development and climate change adaptation. The two primary research objectives can be outlined as follows. Firstly, utilising EO data (specifically HS imagery from the PRISMA satellite) and GIS data to classify urban landscapes into LCZs and analyse their seasonal and spatial dynamics. Secondly, developing high-resolution temperature maps based on in-situ and EO data to identify and quantify UHI across diverse urban contexts.

This paper has been divided into four sections as follows. After the introductory section, Section 2 is concerned with the test sites, data and methods of the research. Section 3 then presents the research findings, including LCZ and air temperature maps and discusses the results. Section 4 describes the project's impact and concludes the work.

1.1 LCZ mapping overview

LCZ mapping is a key area in urban climatology, originating from Stewart and Oke's 2012 study. Initially, LCZs were used to assess the influence of urban morphology on meteorological stations. Over time, the concept has expanded, leading to the development of multiple classification methods. These methods fall into four categories: expert knowledge-based, GIS-based,

Remote Sensing imagery-based, and combined approaches (Lehnert et al., 2021). The expert knowledge-based method relies on local expertise, while the GIS-based method calculates LCZ parameters using GIS tools. Remote Sensing imagery-based methods use satellite imagery to classify LCZs, and combined methods integrate multiple techniques for improved accuracy.

Recently, ML has gained popularity in LCZ classification, particularly within Remote Sensing and combined approaches. MS imagery has been widely used due to its global availability. However, the LCZ-ODC project has demonstrated that HS imagery, when combined with GIS data, enhances classification accuracy—achieving over 85% accuracy in Milan (Vavassori et al., 2024). LCZ-UHI-GEO will continue emphasizing HS data from the PRISMA satellite, using MS imagery for performance comparisons. The integration of advanced satellite data and ML is expected to improve LCZ classification precision further, benefiting urban climate studies worldwide.

1.2 Air temperature mapping overview

The limited number of meteorological stations makes urban heat assessment challenging, leading to increased use of thermal remote sensing and Land Surface Temperature (LST) analysis (Bechtel et al., 2019a). While LST helps detect surface UHI (SUHI), it does not reflect felt temperature, highlighting the need for air temperature mapping. These maps are crucial for analysing microclimatic conditions, heat stress, and thermal comfort, particularly in studying Canopy Layer UHI (CUHI) and urban-rural temperature variations.

Since air temperature is rarely available as a high-resolution spatial product, various methods estimate it where direct measurements are missing, differing in accuracy, resolution, and computational demand (Ding et al. 2023, Hassani et al. 2024, Venter et al., 2020).

The main approaches include: (i) Remote Sensing-Based Methods, which use satellite data like LST (e.g., TVX method) to estimate air temperature; (ii) numerical modelling, which applies physical simulations such as Numerical Weather Prediction (NWP) and Energy Balance models; and (iii) statistical and ML methods, which estimate air temperature with multiple predictors (e.g., elevation, vegetation fraction, sky view factor), using ML algorithms (such as Random Forest and XGBoost) and geostatistical methods (e.g., Inverse Distance Weighting and Kriging).

To improve the interpolation with denser data coverage, crowdsourced networks like Netatmo (Netatmo, 2025) can be integrated with EO data, enabling the creation of more accurate continuous air temperature maps as will be described in detail in the following sections.

2. Data and Methods

2.1 Test sites

UHI has a pronounced effect in cities of all sizes, but its intensity and negative consequences on the population are most pronounced in large cities (Kopec, 1970). Following that, the two biggest cities in both Italy and Vietnam have been selected as test sites for the LCZ-UHI-GEO project. In Italy, the selected cities are Rome and Milan, while in Vietnam they are Hanoi and Ho Chi Minh City.

In these cities, the effects of elevated heat stress are likely to have a significant impact on human well-being due to the high population density. Furthermore, all four cities extend over large areas, are characterised by a high sealed surface ratio, and have complex urban morphological patterns with a variety of LCZs present, making them interesting sites for exploring the UHI-LCZ relationship.

This study presents the preliminary results achieved for the Italian case studies, for which the available high-quality data allowed us to map both LCZ and air temperature. The LCZ mapping methodology is presented for the example of Rome, while air temperature mapping is presented for Milan. Figure 1 shows the area of interest for both cities.

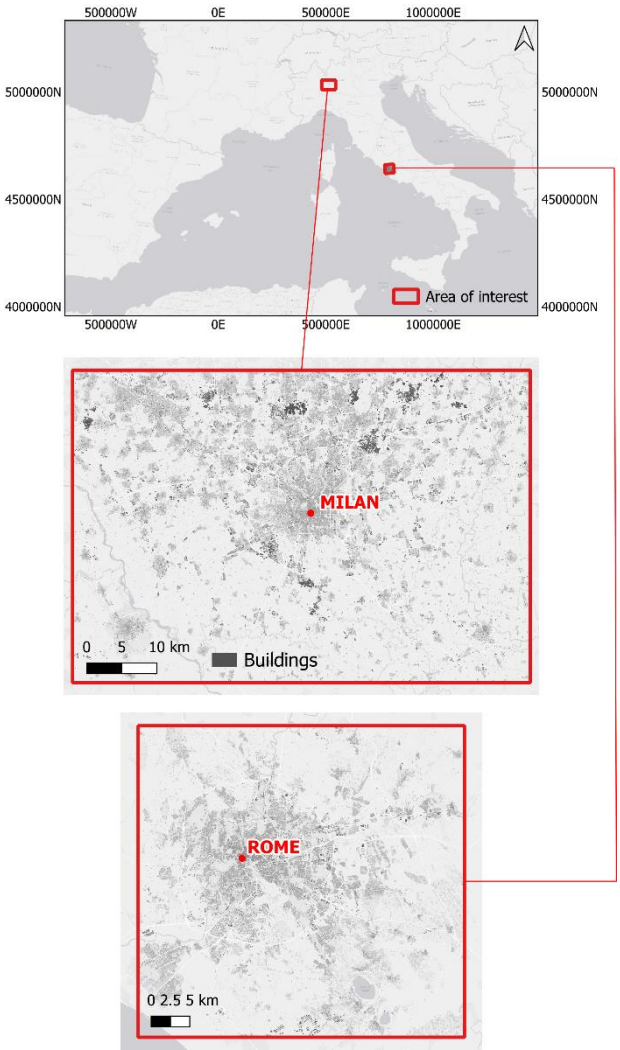

Figure 1. Study sites of the project, Milan (middle) and Rome (bottom), Italy.

2.2 PRISMA data retrieval

Ad hoc PRISMA data license was set up during the early summer of 2024, and PRISMA data collection started in mid-July 2024 for all four cities encompassed in the LCZ-UHI-GEO project. Satellite imagery tasking was conducted using the PRISMA pre-feasibility tool (prisma-prefeasibility.asi.it), identifying PRISMA data take opportunities over the cities of interest. By relying upon this tool, new acquisition requests were submitted via the PRISMA Portal (prisma.asi.it). As of January 2025, 63 requests have been submitted for all four cities, with Vietnamese cities having a higher number of submissions (Figure 2).

Ultimately, six cloud-free images were retrieved for Rome, one for Milan, while three acquisitions over Hanoi are currently under a quality evaluation process. For Ho Chi Minh City, no images were retrieved due to persistent cloud cover. For all cities, data

tasking is still in progress. Moreover, in Vietnam, more stable weather conditions are expected with the dry season (typically between December and March), possibly leading to some cloud-free PRISMA images.

Out of six retrieved images in Rome, two have been selected for LCZ mapping, i.e. those collected on 12th August and 10th September 2024.

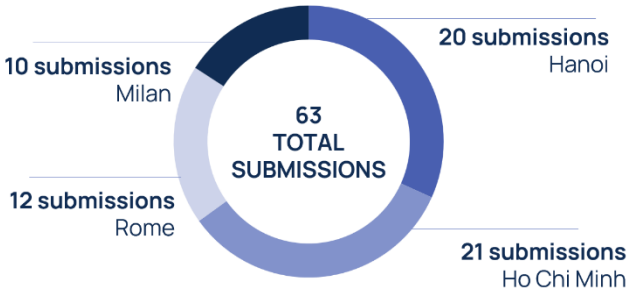

Figure 2. Number of submitted PRISMA data tasking requests between July 2024 and January 2025.

2.3 LCZ Mapping

As mentioned above, LCZ mapping was carried out following the methodology developed within the LCZ-ODC project (Vavassori et al., 2024). Accordingly, PRISMA satellite images were exploited with geospatial data to generate LCZ maps during the summer of 2024 in Rome. Geospatial data corresponds to the so-called Urban Canopy Parameters (UCPs) such as impervious surface fraction, building height, and sky view factor. The full list of UCPs and the source datasets are shown in Table 1. UCPs were normalised in such a way to be comparable with satellite reflectance values. LCZ maps were also generated based on Sentinel-2 imagery for comparative purposes. For that matter, the Sentinel-2 image on 12th August was retrieved from Copernicus Browser (https://browser.dataspace.copernicus.eu/).

LCZ mapping process includes pre-processing satellite images, primarily applying co-registration of PRISMA with Sentinel-2 using the Python package GeFolki. Moreover, Principal Component Analysis (PCA) is applied to PRISMA imagery for dimensionality reduction.

Training and testing LCZ samples are collected, following the LCZ framework. The classification is performed using the Random Forest ML algorithm. The set of features provided as input consists of UCPs and the satellite bands of Sentinel-2 or PCs of PRISMA. Classifier parameters are optimised through cross-validation to improve accuracy. Post-processing involves applying a moving median filter to refine the classified map. Lastly, classification accuracy is evaluated on the testing samples by extracting statistical metrics from the confusion matrix, including overall accuracy (OA), precision, recall and F1-score. This hybrid approach enhances classification reliability by integrating multiple data sources and refining classification parameters.

Table 1. List of UCPs collected for Rome

UCP	DESCRIPTION	SOURCE
BUILDING HEIGHTS	Retrieved from geo-topographic database of Lazio region	LINK
TREE CANOPY HEIGHTS	Global high-resolution (1m) canopy height data based on Maxar imagery	LINK
IMPERVIOUS SURFACE FRACTION	Copernicus Land Monitoring Service (CLMS) dataset on imperviousness density from 2018 (10m)	LINK
BUILDING SURFACE FRACTION	Calculated from geo-topographic database of Lazio region (building footprints)	LINK
SKY VIEW FACTOR	Calculated from ALOS-DSM and geo-topographic database	LINK

2.4 Air Temperature Mapping

Based on Venter et al. (2020), the air temperature mapping method applies the Random Forest ML algorithm and Earth Observation (EO) data to generate high-resolution (30-m) air temperature maps in Milan, Italy during the summer of 2022. The computations are done in Google Earth Engine (GEE), a cloud-based geospatial computing platform (Gorelick et al., 2017). Key predictors include SWIR-1 and SWIR-2 Sentinel-2 bands, elevation, NDVI, soil moisture, sky view factor, and imperviousness, all selected for their influence on temperature. Furthermore, the interpolation targets key diurnal periods, focusing on peak temperature hours and UHI intensity at night. Specific time windows include 4-6 AM (coolest period), 9-11 AM (mid-morning), 2-4 PM (hottest daily), 6-8 PM (early evening), and 9 PM-12 AM (strong UHI intensity).

Unlike Venter's method, which relies solely on Netatmo data, this approach combines Netatmo measurements with the official data from the Regional Environmental Protection Agency (ARPA). ARPA data is available in 10-minute intervals with 25 stations present in the wider surrounding of Milan. It was retrieved from the official ARPA website. Netatmo data was retrieved using a dedicated Netatmo API service and the *patatmo* Python package. Finally, a thorough data-cleaning procedure is applied to Netatmo (Puche et al., 2023).

For the summer of 2022, 641 Netatmo and 25 ARPA stations are available in the area of interest, totalling 666 stations. They were combined and split into training and testing datasets, corresponding to 70% and 30% of the full dataset, respectively. Accordingly, training data consists of 465 stations while testing of 201. As an example, Figure 3 presents the spatial distribution of training and testing points for the diurnal period 4-6 AM.

The predicted air temperature maps for each diurnal period were validated against testing data and evaluated based on the root mean square error (RMSE) metric.

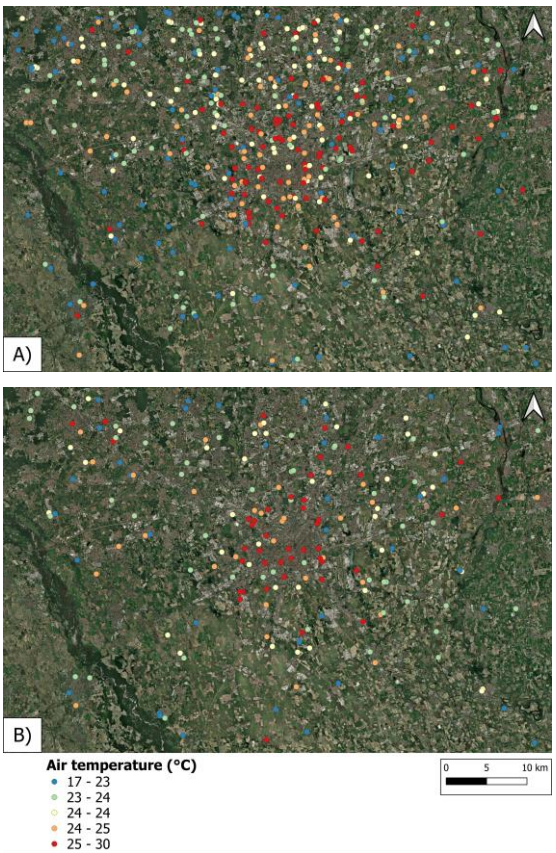

Figure 3. Spatial distribution of training (a) and testing (b) Netatmo/ARPA air temperature datasets in Milan, Italy for 4-6 AM period.

3. Results and discussion

3.1 LCZ Mapping

Figure 4 presents the final LCZ maps generated for August 12th, the date on which both PRISMA and Sentinel-2 imagery were acquired. A strong level of coherence was observed between the two datasets, indicating a generally consistent representation of the mapped LCZs. However, some differences remain, suggesting potential further refinements. In terms of OA, Sentinel-2 achieved a performance of 73.7%, while PRISMA outperformed it, reaching 88.1%, thereby providing an improvement of 14.4%. Additionally, the PRISMA image from September 10th also achieved a high level of accuracy, at 85.6%. Hence, all images achieved an OA above the threshold of 50%. This threshold was proposed by Bechtel et al. (2019b) and describes an appropriate benchmark to pass the quality control, meaning that all maps can be considered reliable.

Sentinel-2 and PRISMA satellite imagery reveal a generally similar spatial pattern of LCZs; however, some differences exist due to the spectral variations between the two sensors.

LCZs in Rome highlight the city's specific urban structure. The historic city centre is predominantly compact, with a concentration of high-density built-up LCZs, mainly LCZ 2 (Compact mid-rise) and LCZ 3 (Compact low-rise). Such densely built-up centres are characteristic of European cities of old foundation. However, Rome also exhibits a high presence of high-rise LCZs, LCZ 1 (Compact high-rise) and LCZ 4 (Open high-rise) which are typically less common in European urban areas. Surrounding the central core are neighbourhoods with lower density, where LCZ 5 (Open mid-rise) and LCZ 6 (Open low-rise) dominate, creating a transition between the densely built centre and the more suburban periphery. Rome also has extensive industrial zones, particularly on its eastern side, where LCZ 8 (Large low-rise) is highly prevalent.

Natural LCZs are important in Rome's urban climate. Dense tree cover (LCZ A) is mainly concentrated in the southeastern part of the city, but several large urban parks closer to the city core are also present. These urban green areas can contribute significantly to the cooling effect (Taha, 1997; Yu et al., 2020). One of the most significant examples is Villa Borghese, the largest central green area, which provides support against negative UHI effects such as heightened temperatures. Despite these green spaces, they still make up a small fraction of central Rome, and the biggest area belongs to urban LCZs.

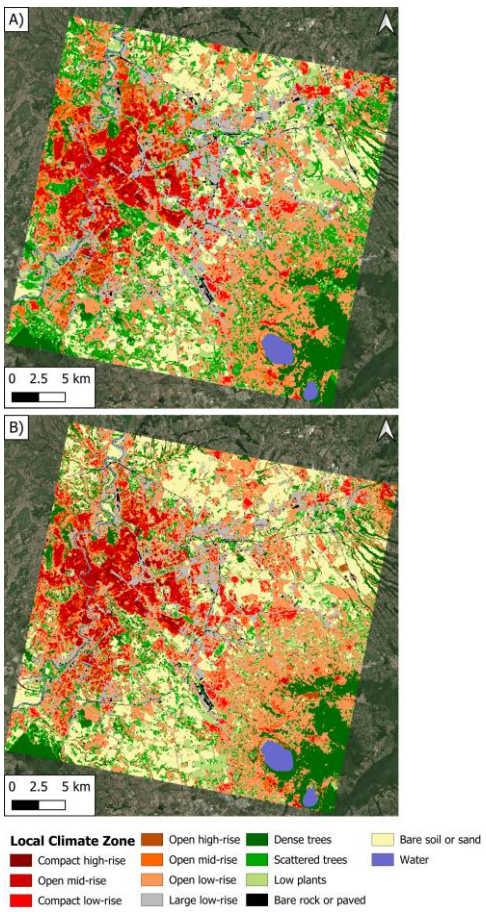

Figure 4. LCZ maps of Rome, Italy based on PRISMA (a) and Sentinel-2 (b) for 12th August 2024.

Furthermore, a substantial portion of the area of interest surrounding Rome is classified as LCZ F (Bare soil or sand). This can be attributed to Rome's southern geographical location, where dry summer conditions and extensive agricultural activity in surrounding areas contribute to large bare land surfaces and the fact that the PRISMA image used for classification was collected in the hottest summer ever recorded over the past century (C3S, 2024). In some cases, this can result in a reverse UHI effect, where the rural surroundings can be equally or even hotter than the central urban area (Stroppiana et al., 2014). Moreover, this influences the limited presence of LCZ D (Low plants) during August in Rome. However, in wetter months when dry soils are replaced with green fields, LCZ D might be more prevalent. This further suggests that natural LCZs are the most dynamic over time and that they require careful analysis to accurately capture their variations (Geletič et al., 2019). Hence, a multi-temporal LCZ classification approach should be followed.

3.2 Air temperature mapping

Figure 5 shows interpolated air temperature maps using Random Forest ML regression averaged over the summer of 2022. Each diurnal period is presented and points out a specific spatio-temporal change in air temperatures.

Models were validated based on the test dataset (Figure 3b). The validation results indicate a good performance of the model, with an average RMSE of 1.4 °C across all periods (Table 2). The best performance is observed for the evening and night-time hours, at 1.3 °C. However, the differences between periods are not large, indicating that the model performs well for all the hours. Additionally, the range is greatest during night-time hours, specifically 4-6 AM and 9 PM-12 AM, suggesting more significant spatial variations in air temperature distribution. In contrast, the smallest range occurs during the evening and daytime values, ranging from 3.6 to 4.2 °C. This implicates a more stable spatial pattern of air temperature.

Table 2. Range and RMSE values of interpolated maps for each diurnal period

Time	Range (°C)	RMSE (°C)
4-6 AM	5.8	1.3
9-11 AM	3.6	1.5
2-4 PM	4.2	1.4
6-8 PM	3.7	1.3
9 PM – 12 AM	5.5	1.3

When observing the daily development of air temperature, one can notice a much more emphasised UHI pattern during night-time hours, i.e. 4-6 AM and 9 PM-12 AM (Figure 5a, e). For those hours, the central urban areas experience much higher air temperatures compared to their surroundings. A similar pattern can be observed also for the evening period, between 6-8 PM (Figure 5d), however with slightly lower intensity. Such stronger UHI is the consequence of the heat retention properties of urban surfaces. During the day, materials like concrete, asphalt, and buildings absorb and store heat, releasing it slowly after sunset (Oke et al., 2017). In contrast, rural areas with more vegetation and open soil surfaces cool down more rapidly due to higher evapotranspiration and lower heat storage capacity. Furthermore, the absence of solar radiation during the night leads to a more stable urban atmosphere in terms of atmospheric mixing. This allows urban areas to retain the heat while rural areas cool down significantly. Consequently, the interpolated maps for night-time demonstrate a larger range than during daytime. This is also true for the 6-8 PM period when the cooling phase has just started, and the differences are smaller.

During the daytime, for the period 9-11 AM, the central area remains warmest, however, the city’s surroundings also begin to heat up (Figure 5b). These areas of elevated air temperature in the surroundings correspond to bare soils, which can absorb a large amount of incoming solar radiation. As the day continues, temperatures continue to rise and are warmest for the period 2-4 PM (Figure 5c). Then, air temperatures can reach up to 33 °C. However, it is noticeable that the urban core is no longer the warmest area, but that certain rural areas experience higher values. This phenomenon, known as “cool island” (Chen et al., 2014) occurs during the daytime, particularly in the cities surrounded by extensive bare soils. The unique thermal characteristics of bare soils influence high temperatures leading to an inversion of the typical UHI pattern.

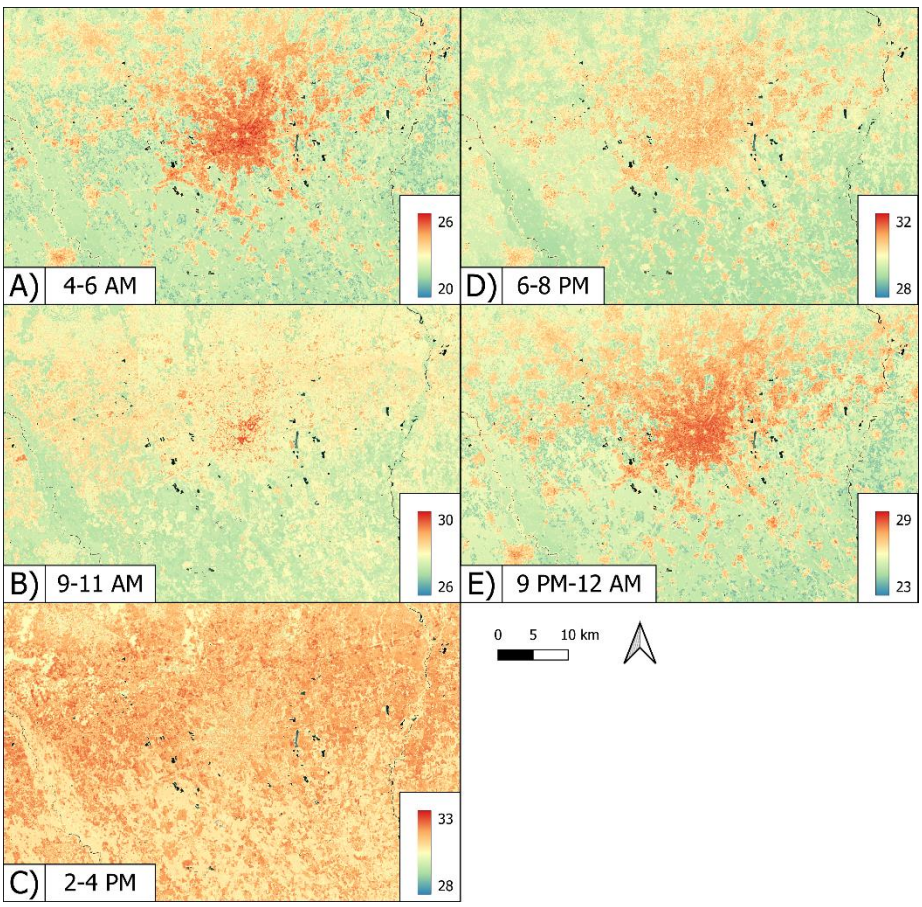

Figure 5. Interpolated air temperature maps (°C) for summer 2022 (June, July, August) for multiple diurnal periods: 4-6 AM (a), 9-11 AM (b), 2-4 PM (c), 6-8 PM (d), 9 PM-12 AM (e). *Note: For improved readability, each map has a unique colour ramp temperature range.*

https://doi.org/10.5194/isprs-archives-XLVIII-G-2025-1685-2025

4. Conclusions

This paper aimed to examine the effectiveness of geospatial techniques in mapping LCZs and air temperature using advanced geospatial techniques. Through the integration of HS data from the PRISMA satellite and high-resolution EO datasets, this study successfully demonstrated methodologies for urban climate analysis in two major Italian cities, i.e. Rome and Milan. Moreover, we aim to extend its analysis to two Vietnamese cities, Hanoi and Ho Chi Minh City in the next phases of the LCZ-UHI-GEO project.

The LCZ mapping method was based on the combination of UCPs and PRISMA imagery, utilising the Random Forest ML algorithm for classification in Rome. The findings indicate that the use of PRISMA HS imagery significantly enhances LCZ classification accuracy, achieving 88.1%, compared to 73.7% obtained with Sentinel-2 data. These results highlight the added value of high spectral resolution in mapping LCZs. Furthermore, they provide accurate insights into the distribution of LCZs in Rome, supporting the next steps of urban climate research.

The second aim of this study was to investigate the air temperature mapping approach, which combined ML-based interpolation with in-situ and EO data in Milan. We set out to predict continuous air temperature space-time patterns, providing high-resolution temperature maps. The interpolation was focused on multiple diurnal periods for the summer of 2022. The model shows good performance with an average RMSE of 1.4°C across all diurnal periods. Additionally, the results revealed changing temperature patterns, with pronounced UHI occurring during night-time when temperature differences between the urban core and surrounding rural areas are highest. In contrast, during the warmest time of the day, between 2-4 PM, a slight cool island effect forms. These new findings should assist in our understanding of the temporal dynamics of UHI.

For future work, PRISMA data acquisition will be continued to obtain the highest possible amount of HS imagery, supporting LCZ mapping. Interpolating air temperatures during heat waves will provide insights into extreme urban heat patterns and their spatial variations, aiding the assessment of urban heat stress. Additionally, multi-temporal LCZ mapping will be further refined for all cities, with a particular focus on Vietnamese sites where data availability is lacking. Furthermore, complex urban fabrics and rapid urbanisation in Vietnam present challenges requiring methodological improvements.

In conclusion, as urbanisation accelerates and climate-related risks intensify, initiatives such as the LCZ-UHI-GEO project are essential in collecting scientific evidence to inform climate resilience through geospatial research. Also, the outputs of this project will be shared with stakeholders and decision-makers to aid urban planning and policymaking. The project also facilitates knowledge exchange, skill transfer, and capacity building through workshops and stakeholder engagement activities. Through geospatial research and innovation, LCZ-UHI-GEO utilises data-driven solutions to address climate change challenges and promote sustainable urban development and climate resilience.

Acknowledgements

This study is part of the LCZ-UHI-GEO project (ID PGR12284), funded by the Italian Ministry of Foreign Affairs and International Cooperation (MAECI) and Vietnam's Ministry of Science and Technology (MOST).
Part of this study is based on the methodology developed within the LCZ-ODC project, funded by the Italian Space Agency (agreement n. 2022-30-HH.0) in the framework of the "Innovation for Downstream Preparation for Science (I4DP_SCIENCE)" program.

References

Bechtel, B., Demuzere, M., Mills, G., Zhan, W., Sismanidis, P., Small, C., & Voogt, J. (2019a). SUHI analysis using local climate zones—A comparison of 50 cities. Urban Climate, 28, 100451. https://doi.org/10.1016/j.uclim.2019.01.005

Bechtel, B., Alexander, P. J., Beck, C., Böhner, J., Brousse, O., Ching, J., ... & Xu, Y. (2019b). Generating WUDAPT Level 0 data–Current status of production and evaluation. Urban climate, 27, 24-45. https://doi.org/10.1016/j.uclim.2018.10.001

Chapman, S., Watson, J. E. M., Salazar, A., Thatcher, M., & McAlpine, C. A. (2017). The impact of urbanization and climate change on urban temperatures: A systematic review. Landscape Ecology, 32, 1921–1935. https://doi.org/10.1007/s10980-017-0561-4

Chen, A., Yao, X. A., Sun, R., & Chen, L. (2014). Effect of urban green patterns on surface urban cool islands and its seasonal variations. Urban forestry & urban greening, 13(4), 646-654. https://doi.org/10.1016/j.ufug.2014.07.006

Copernicus Climate Change Service (C3S), August 2024 Climate Bulletin: Summer 2024 – Hottest on record globally and for Europe. https://climate.copernicus.eu/copernicus-summer-2024-hottest-record-globally-and-europe (accessed 10 February 2025)

Ding, X., Zhao, Y., Fan, Y., Li, Y., & Ge, J. (2023). Machine learning-assisted mapping of city-scale air temperature: Using sparse meteorological data for urban climate modeling and adaptation. Building and Environment, 234, 110211. https://doi.org/10.1016/j.buildenv.2023.110211

Geletič, J., Lehnert, M., Savić, S., & Milošević, D. (2019). Inter-/intra-zonal seasonal variability of the surface urban heat island based on local climate zones in three central European cities. Building and Environment, 156, 21-32. https://doi.org/10.1016/j.buildenv.2019.04.011

Gorelick, N., Hancher, M., Dixon, M., Ilyushchenko, S., Thau, D., & Moore, R. (2017). Google Earth Engine: Planetary-scale geospatial analysis for everyone. Remote sensing of Environment, 202, 18-27. https://doi.org/10.1016/j.rse.2017.06.031

Hassani, A., Santos, G. S., Schneider, P., & Castell, N. (2024). Interpolation, satellite-based machine learning, or meteorological simulation? A comparison analysis for spatio-temporal mapping of mesoscale urban air temperature. Environmental Modeling & Assessment, 29(2), 291-306. https://doi.org/10.1007/s10666-023-09943-9

Kopec, R. J. (1970). Further observations of the urban heat island in a small city. Bulletin of the American Meteorological Society, 51(7), 602-607. https://doi.org/10.1175/1520-0477(1970)051%3C0602:FOOTUH%3E2.0.CO;2

Lehnert, M., Savic, S., Milosevic, D., Dunjic, J., Geletic, J., 2021. Mapping local climate zones and their applications in European

urban environments: a systematic literature review and future development trends. ISPRS Int. J. Geo Inf. 10, 260. https://doi.org/10.3390/ijgi10040260

Netatmo – Official Weather Map.
https://weathermap.netatmo.com/ (accessed 27 January 2025)

Oke, T.R., Mills, G., Christen, A., & Voogt, J. (2017). Urban climates. Cambridge University Press.

Puche, M., Vavassori, A., & Brovelli, M. A. (2023). Insights into the effect of urban morphology and land cover on land surface and Air temperatures in the metropolitan city of milan (Italy) using satellite imagery and In situ measurements. Remote Sensing, 15(3), 733.
https://doi.org/10.3390/rs15030733

Stewart, I.D., Oke, T.R., 2012. Local climate zones for urban temperature studies. Bull. Am. Meteorol. Soc. 93. https://doi.org/10.1175/BAMS-D-11-00019.1

Stroppiana, D., Antoninetti, M., & Brivio, P. A. (2014). Seasonality of MODIS LST over Southern Italy and correlation with land cover, topography and solar radiation. European Journal of Remote Sensing, 47(1), 133-152. https://doi.org/10.5721/EuJRS20144709

Taha, H. (1997). Urban climates and heat islands: Albedo, evapotranspiration, and anthropogenic heat. Energy and Buildings, 25, 99–103.
https://doi.org/10.1016/S0378-7788(96)00999-1

Vavassori, A., Oxoli, D., Venuti, G., Brovelli, M. A., de Cumis, M. S., Sacco, P., & Tapete, D. (2024). A combined Remote Sensing and GIS-based method for Local Climate Zone mapping using PRISMA and Sentinel-2 imagery. International Journal of Applied Earth Observation and Geoinformation, 131, 103944. https://doi.org/10.1016/j.jag.2024.103944

Venter, Z. S., Brousse, O., Esau, I., & Meier, F. (2020). Hyperlocal mapping of urban air temperature using remote sensing and crowdsourced weather data. Remote Sensing of Environment, 242, 111791.
https://doi.org/10.1016/j.rse.2020.111791

Yu, Z., Yang, G., Zuo, S., Jørgensen, G., Koga, M., & Vejre, H. (2020). Critical review on the cooling effect of urban blue-green space: A threshold-size perspective. Urban for Urban Green, 49, 126630. https://doi.org/10.1016/J.UFUG.2020.126630